

Article

Differential Chemical Profile of Metabolite Extracts Produced by the *Diaporthe citri* (G-01) Endophyte Mediated by Varying the Fermented Broth pH

Julio Cesar Polonio ^{1,*}, Marcos Alessandro dos Santos Ribeiro ^{1,2}, Cintia Zani Fávaro-Polonio ¹, Eduardo Cesar Meurer ² , João Lúcio Azevedo ³ , Halison Correia Golias ¹  and João Alencar Pamphile ^{1,†}

¹ Laboratory of Microbial Biotechnology LBIOMIC/UEM, Departamento de Biotecnologia Genética e Biologia Celular, Universidade Estadual de Maringá, Maringá 87020-900, PR, Brazil;

marcosquimicauem@hotmail.com (M.A.d.S.R.); cintiazanifavaropolonio@gmail.com (C.Z.F.-P.); halisongolias@utfpr.edu.br (H.C.G.)

² Laboratory of Mass Spectrometry “LabFenn”, Campus de Jandaia do Sul, Universidade Federal do Paraná, Jandaia do Sul 86900-000, PR, Brazil; eduardo.meurer@ufpr.br

³ Departamento de Genética, Escola Superior de Agricultura “Luiz de Queiroz”—USP, Piracicaba 13418-900, SP, Brazil; jlazevedo@usp.br

* Correspondence: jcpolonio2@uem.br; Tel.: +55-44-3011-4683 or +55-44-99848-1990

† In memoriam.



Citation: Polonio, J.C.; Ribeiro, M.A.d.S.; Fávaro-Polonio, C.Z.; Meurer, E.C.; Azevedo, J.L.; Golias, H.C.; Pamphile, J.A. Differential Chemical Profile of Metabolite Extracts Produced by the *Diaporthe citri* (G-01) Endophyte Mediated by Varying the Fermented Broth pH. *Metabolites* **2022**, *12*, 692. <https://doi.org/10.3390/metabo12080692>

Academic Editor: Cecília R.C. Calado

Received: 4 June 2022

Accepted: 21 July 2022

Published: 26 July 2022

Publisher’s Note: MDPI stays neutral with regard to jurisdictional claims in published maps and institutional affiliations.



Copyright: © 2022 by the authors. Licensee MDPI, Basel, Switzerland. This article is an open access article distributed under the terms and conditions of the Creative Commons Attribution (CC BY) license (<https://creativecommons.org/licenses/by/4.0/>).

Abstract: Endophytic microorganisms show great potential for biotechnological exploitation because they are able to produce a wide range of secondary compounds involved in endophyte–plant adaptation, and their interactions with other living organisms that share the same microhabitat. Techniques used to chemically extract these compounds often neglect the intrinsic chemical characteristics of the molecules involved, such as the ability to form conjugate acids or bases and how they influence the solubilities of these molecules in organic solvents. Therefore, in this study, we aimed to evaluate how the pH of the fermented broth affects the process used to extract the secondary metabolites of the *Diaporthe citri* strain G-01 endophyte with ethyl acetate as the organic solvent. The analyzed samples, conducted by direct-infusion electrospray-ionization mass spectrometry, were grouped according to the pH of the fermented broth (i.e., <7 and ≥7). A more extreme pH (i.e., 2 or 12) was found to affect the chemical profile of the sample. Moreover, statistical analysis enabled us to determine the presence or absence of ions of high importance; for example, ions at 390.7 and 456.5 *m/z* were observed mainly at acidic pH, while 226.5, 298.3, and 430.1 *m/z* ions were observed at pH ≥ 7. Extraction at a pH between 4 and 9 may be of interest for exploring the differential secondary metabolites produced by endophytes. Furthermore, pH influences the chemical phenotype of the fungal metabolic extract.

Keywords: principal component analysis; endophytes; DI-ESI-MS; multivariate statistics; secondary metabolites

1. Introduction

Endophytic microorganisms are being increasingly studied; of the more than one million published papers, 40,000 have focused on chemically characterizing compounds produced by these organisms [1]. The ability to establish symbiotic relationships with plant tissue and organs in extremely specific microhabitats is frequently provided as the rationale for exploring this ecological niche [2].

Chemical, physical, and genetic factors determined whether or not an endophyte is established, with the endophyte and host plant required to develop a balanced symbiotic relationship [3]. Endophytes can influence plant metabolism, plants can promote microbial metabolism, and both organisms may be responsible for specific metabolic pathways. Furthermore, plants can metabolize compounds produced by endophytes, and vice versa [4].

This complex network of chemical communication and metabolic activity between organisms produces new natural compounds with antifungal, antibacterial, and/or antitumor activities [5–12]. Between 2012 and 2014, Chagas et al. [7] reported more than 300 new metabolic compounds produced by endophytes.

Compounds produced by endophytes include a broad range of structural groups, including benzopyranones, cytochalasins, quinones, steroids, isocoumarins, terpenoids, and others [5,6,13–19]. Moreover, these microorganisms can produce the same or mimetic compounds derived from the host plant, thereby potentially facilitating the production of metabolic compounds in industrial bioreactors. Indeed, this method has been used to prepare paclitaxel, an antitumor compound produced by *Taxomyces andreanae* isolated from *Taxus brevifolia* [5]. Although properly domesticating endophytes for industrial production remains difficult [20], the discovery of this compound is one of the main reasons for the accelerated exploration of metabolites produced by endophytes.

Endophyte metabolites are routinely studied using axenic endophytic cultures followed by growth in artificial broths and secondary-metabolite extraction by partitioning with organic solvents [1,21–26]. The crude extracts are then subjected to analysis and chromatographic separation to produce fractions with higher degrees of purification prior to being chemically analyzed using techniques such as nuclear magnetic resonance (NMR) spectroscopy and/or mass spectrometry (MS) for chemical annotation [23,27–29].

Frequent re-isolation and re-characterization of known compounds is a current problem confronted by natural-compound studies. Therefore, new approaches that more easily discriminate between known molecules and new compounds are needed [29]. In addition to chemical-identification techniques, inducing differential secondary metabolic pathways and extraction methods is an approach that can be better exploited [1,4,30,31]. Chemical-composition data can be applied to fungal chemotaxonomic approaches, as reported by Mácia-Vicente et al. [29], who studied the chemical profiles of more than 800 strains, annotated more than 1000 compounds, and identified compounds exclusively found in specific orders.

The solubility of a substance in a solvent is a chemical characteristic that is often overlooked; this qualitative attribute is directly related to molecular structure, especially the polarities of chemical bonds and the chemical species as a whole (dipole moment). Organic compounds may be present as apolar species that are insoluble in water, or they may display alternative polarities and solubilities in various solvents, and at different temperatures and pH values. In addition, functional groups may favor dipole–dipole interactions [32]. Moreover, the molecule may exist as its conjugate acid or base in solution, which influences its solubilities [33]. Consequently, the constitution of a metabolic extract is influenced by pH; consequently, pH is expected to affect the exploration of natural-compound and chemotaxonomic studies.

In this study, we used direct-infusion electrospray-ionization mass spectrometry (DI-ESI/MS) to evaluate how varying the pH following incubation (but before the organic solvent partition step) affects the chemical profiles of endophyte extracts [34], with the data subsequently analyzed using multivariate statistical approaches. This study aimed to demonstrate that the chemical-profile data obtained by DI-ESI/MS show patterns that depend on pH when metabolites are extracted from the same fermented broth using the same microbial strain. This approach may result in liquid–liquid extraction protocols exhibiting higher molecular richness, and provide other poorly soluble molecules using specific solvents and conditions, such as the pH at the end of the fermentation process.

2. Results and Discussion

The WV extracts (see Material and Methods section for descriptions of the “WV”, “PV”, and “MV” extract terminology) provided higher yields than the other solvent protocols used in this study (Figure 1), with the highest yields obtained at pH < 7. All treatment protocols provided higher yields than that containing only broth culture medium (blank,

B). The mean yield obtained at pH 4 by WV treatment is equivalent to that previously reported [34], demonstrating that the extraction method is experimentally producible.

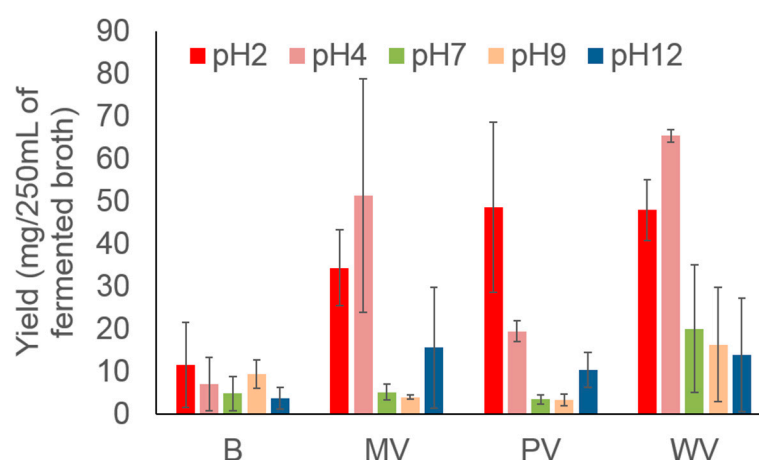


Figure 1. Yields of secondary metabolites extracted using the pH-variation method.

Metabolomics studies that use mass spectrometry generate immense amounts of raw data, and a substantial portion must be initially filtered to obtain concise data prior to any detailed analyses [35,36]. Therefore, we adopted threshold and exclusion peak lists to filter data obtained by analyzing extracts, which helped to exclude background noise signals and mobile phase peaks. The raw data were processed using the MarkerLynx XS software, which led to 86 ions observed in negative mode and 166 in positive mode.

After normalization using the Pareto scale, the data were subjected to ANOVA followed by Tukey's honestly significant difference post hoc test using the MetaboAnalyst platform, which led to 140 ions in positive mode and 77 ions in negative mode, with significant differences observed among samples. Three groups were identified based on the sample distribution provided by principal components analysis (PCA) (Figures 2 and 3), namely, B, and samples with $\text{pH} < 7$, and ≥ 7 . Consequently, we confirmed and defined the three groups/clusters using k-means, with samples compared and grouped into these three clusters.

In positive mode (Figure 2), PCA revealed that for principal components PC1—three represent 31.9%, 11.7%, and 10.8% of the variance, respectively. The bi-plot graph shows that some ions, such as those at 257.8 and 358.0 m/z , are related to PC1 and 2; in contrast, the 226.5 m/z ion is more representative of PC1. K-means clustering revealed an intraspecific predominance among samples with $\text{pH} < 7$ (Cluster 2) and samples with $\text{pH} \geq 7$ (Cluster 1), with all B samples well grouped (Cluster 3). PC1 and PC2 revealed that Clusters 2 (mainly $\text{pH} \geq 7$ samples) and 3 (B) overlap; however, this was overcome by analyzing PC3 (see Supplementary Materials). Nevertheless, two blanks with pH 2 and the PV12 sample remained clustered together with the $\text{pH} < 7$ samples in Cluster 2, and therefore appeared as outliers.

Groups were more distinct in negative mode (Figure 3) than in positive mode. The separation provided by PC1 (with 32.9% of the explained variance) and PC2 (14.2%) enabled k-means to define the clusters well. As demonstrated by loadings analysis, some ions were better a representation for the PCs, namely, those at 203.9 and 240.8 m/z for PC1, and at 549.2 m/z for PC2.

Similar results were observed using the k-means approach during hierarchical cluster analysis (HCA) based on the Euclidian distance method and the Ward grouping algorithm (Figure 4). The B2 and PV12 samples were again grouped at $\text{pH} < 7$ in positive mode, with other groups well-resolved.

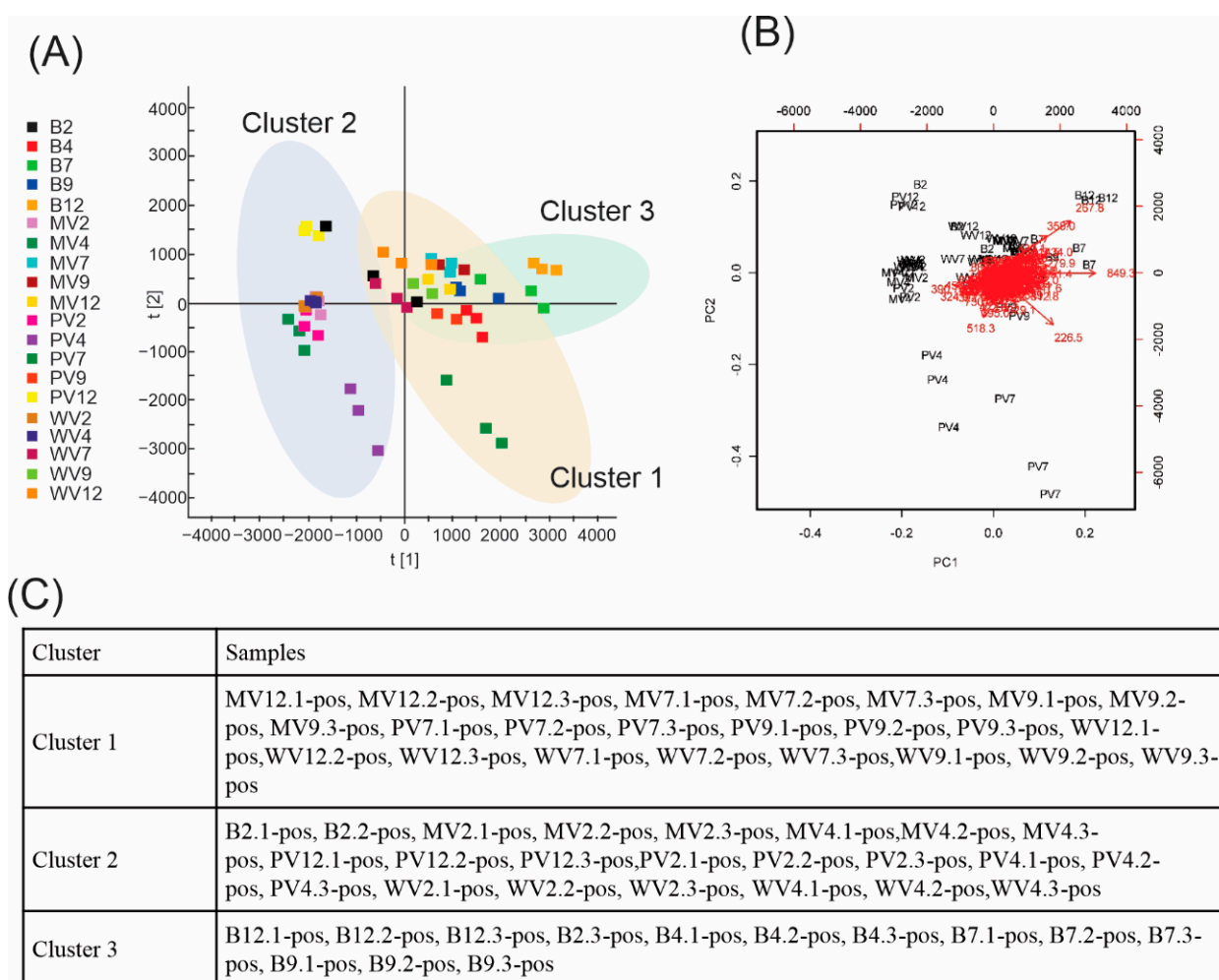


Figure 2. Unsupervised analyses of data acquired in positive mode: **(A)** Principal components analyses (PCAs)—symbols within the delimited transparent areas are those that form clusters defined by k-means. **(B)** Bi-plot analysis (scores \times loadings). **(C)** K-means clusters.

Minimal differences were observed between WV4, PV2, WV2, and MV4 in negative acquisition mode; however, as was previously observed, three clusters (B, $\text{pH} < 7$, and ≥ 7) appeared in well-defined clades. Overall, when compared to the PCA results, those obtained by HCA show global differences among the three clusters in both positive and negative acquisition modes.

Partial least-squares-discriminant analysis (PLS-DA) provided evidence of possible similarities or specific differences through the preferential organization of PCs that are correlated using classificatory variables of interest (i.e., B, $\text{pH} < 7$, and $\text{pH} \geq 7$). While this method separated the samples into the above groups, in negative mode, HCA revealed a group formed by PV4 and MV2 that is slightly different to the other $\text{pH} < 7$ samples. PLS-DA loading analysis showed that two ions are more differentiated for these samples, namely, those at 150.7 and 240.8 m/z . This method generated eight components, where the first three had R^2 and Q^2 values of 0.76 and 0.61, respectively, using the leave-one-out cross-validation (LOOCV) method. These R^2 and Q^2 values indicate that the model exhibits promising data-adjustment and prediction quality [37]. These results were similar to those obtained in positive mode. As was observed using HCA, B2 and PV12 displayed unexpected behavior, with the first three components exhibiting R^2 and Q^2 values of 0.81 and 0.62, respectively (see Supplementary Materials).

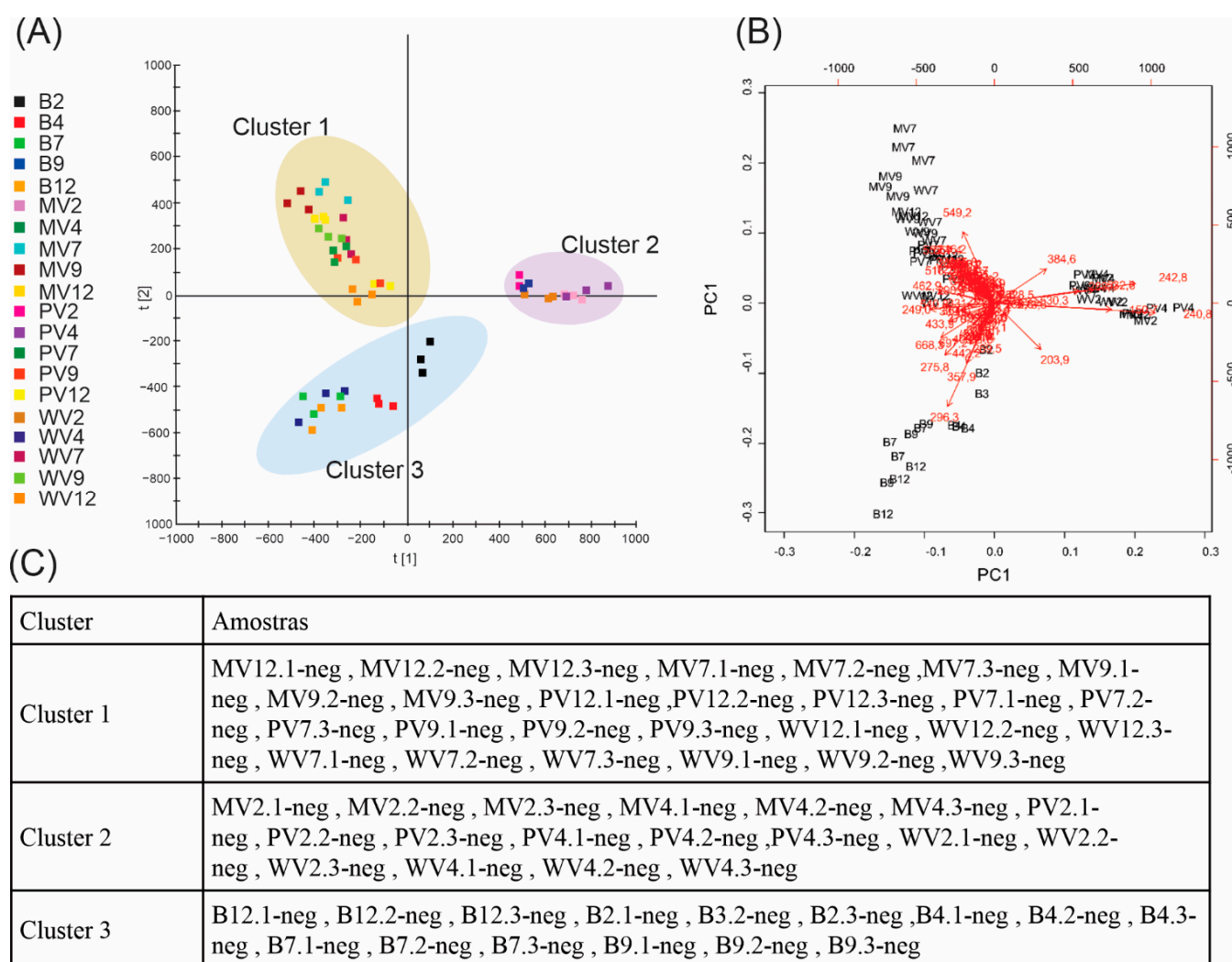


Figure 3. Unsupervised analyses of data acquired in negative mode: (A) Principal components analyses (PCAs)—symbols within the delimited transparent areas are those that form clusters defined by k-means. (B) Bi-plot analysis (scores \times loadings). (C) K-means clusters.

Figures S13 and S14 (Supplementary Materials) present the top 25 variable influences on projection (VIPs) ions defined by PLS-DA. The chemical profiles of the treated samples acquired in positive acquisition mode are graphically summarized. B2 and PV12 display patterns that are incompatible with the other sample groups, from which we infer that extreme pH variations (i.e., 2 or 12) favor unpredictable chemical reactions; although, we do not have prior knowledge of the exact chemical constitution of the extract [38]. Similar observations are made for other samples at pH 2 and 12, but they are less notable than those made for B2 and PV12. Based on the data acquired using the negative method, we conclude that principal ions are well defined in the $\text{pH} < 7$ samples, but a few discrepancies are observed for the B and $\text{pH} \geq 7$ samples.

The orthogonal partial-least-squares discriminant analysis (OPLS-DA) approach was applied to reveal the main differences between sample groups generated by k-means (specifically, comparison between Clusters 1 and 2 using both acquisition methods; see Supplementary Materials). The B clusters were not analyzed because we aimed only to identify differences caused by varying the pH. Figure 5A shows the S-plot ion distributions for the Cluster 1 and 2 samples in positive mode, as generated by MarkerLynx XS. The 390.7, 456.5, and 546.5 m/z ions stand out in the case of Cluster 1, while the others are more notable for Cluster 2. In negative mode (Figure 5B), samples with $\text{pH} < 7$ (Cluster 2) exhibited fewer

ions than those in Cluster 1. These findings suggest that the signs of the ions may have intensified and, consequently, they were highlighted as being more statistically important for group separation.

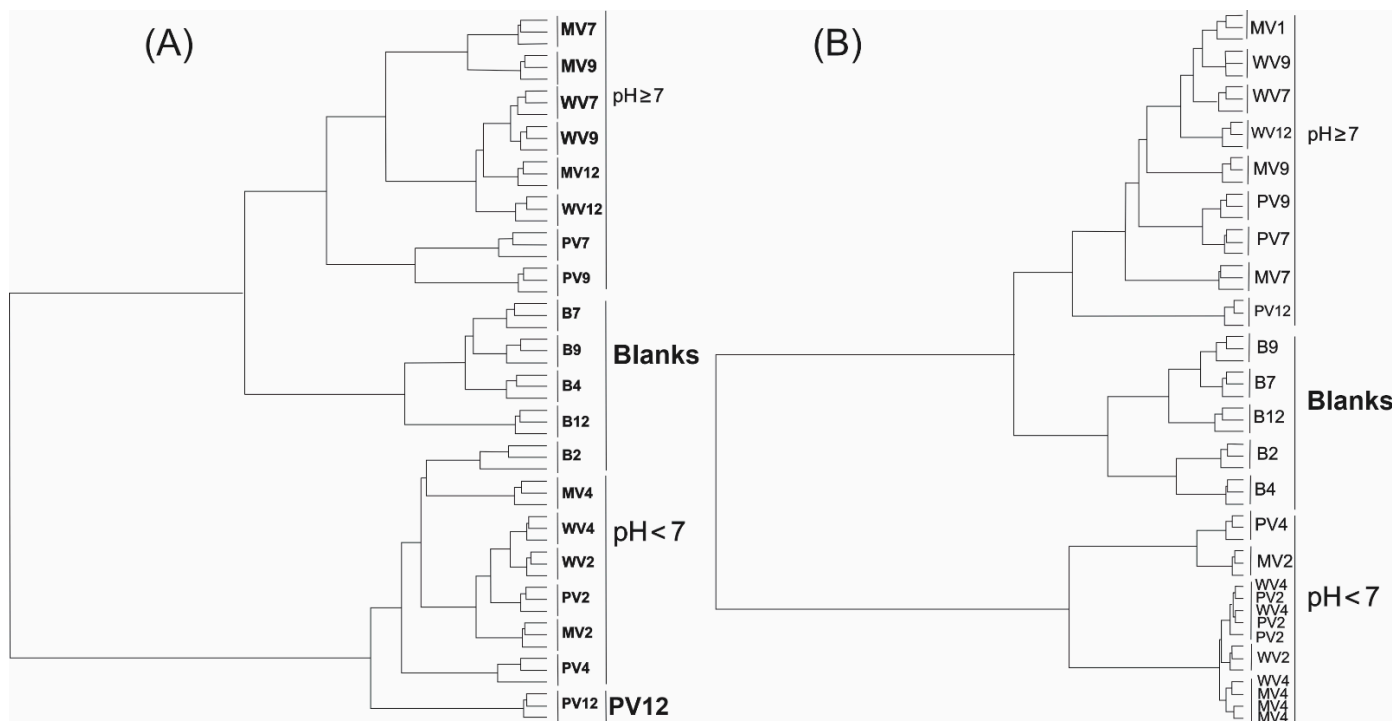


Figure 4. Hierarchical clustering analysis (HCA). Dendrograms were generated by Euclidian distancing and the Ward grouping algorithm for (A) samples obtained in positive acquisition mode and (B) samples obtained in negative acquisition mode.

Nielsen and Larsen [33] showed that pH is an important organic-extraction parameter because more ionizing molecules are extracted into the organic phase at neutral pH than charged ones. Furthermore, most fungal metabolites are acidic; hence, a low pH is sometimes required for extraction [39].

Possible favorable chemical reactions are a major problem associated with the addition of acid or base. For example, alcohols can form esters or lactones with carboxylic acids under acidic conditions [38]. For this reason, extracting natural compounds under extreme pH conditions is of little interest because they are unpredictable (as observed for samples extracted at pH 2 and 12).

Figure 5 shows that experimental design is important when acidifying and/or basifying fermented broths prior to organic solvent partitioning. Ions at 390.7 and 456.5 m/z that appeared mainly under acidic conditions, and ions at 226.5, 298.3, and 430.1 m/z observed at $pH \geq 7$ are the most important differences observed between extracts.

The literature appears to lack studies that consider the pH of the fermented broth when characterizing metabolomic profiles, with process optimization that enables specific compounds to be obtained and purified following fermentation, which is frequently the focus of these studies. For example, Li et al. [40] reported a one-step recovery system for succinic acid from the fermented broth of *Actinobacillus succinogenes* in which adjusting the conditions to acidic pH is a crucial factor in the process because it reduces the solubility of the compound in solution, thereby improving the separation and purification of the product. These achievements rely on the physicochemical characteristics of the molecule of interest, which is present in its acidic form or succinate salt in the fermented broth; the molecule is in its acidic form at pH values below 2.0 and is poorly soluble.

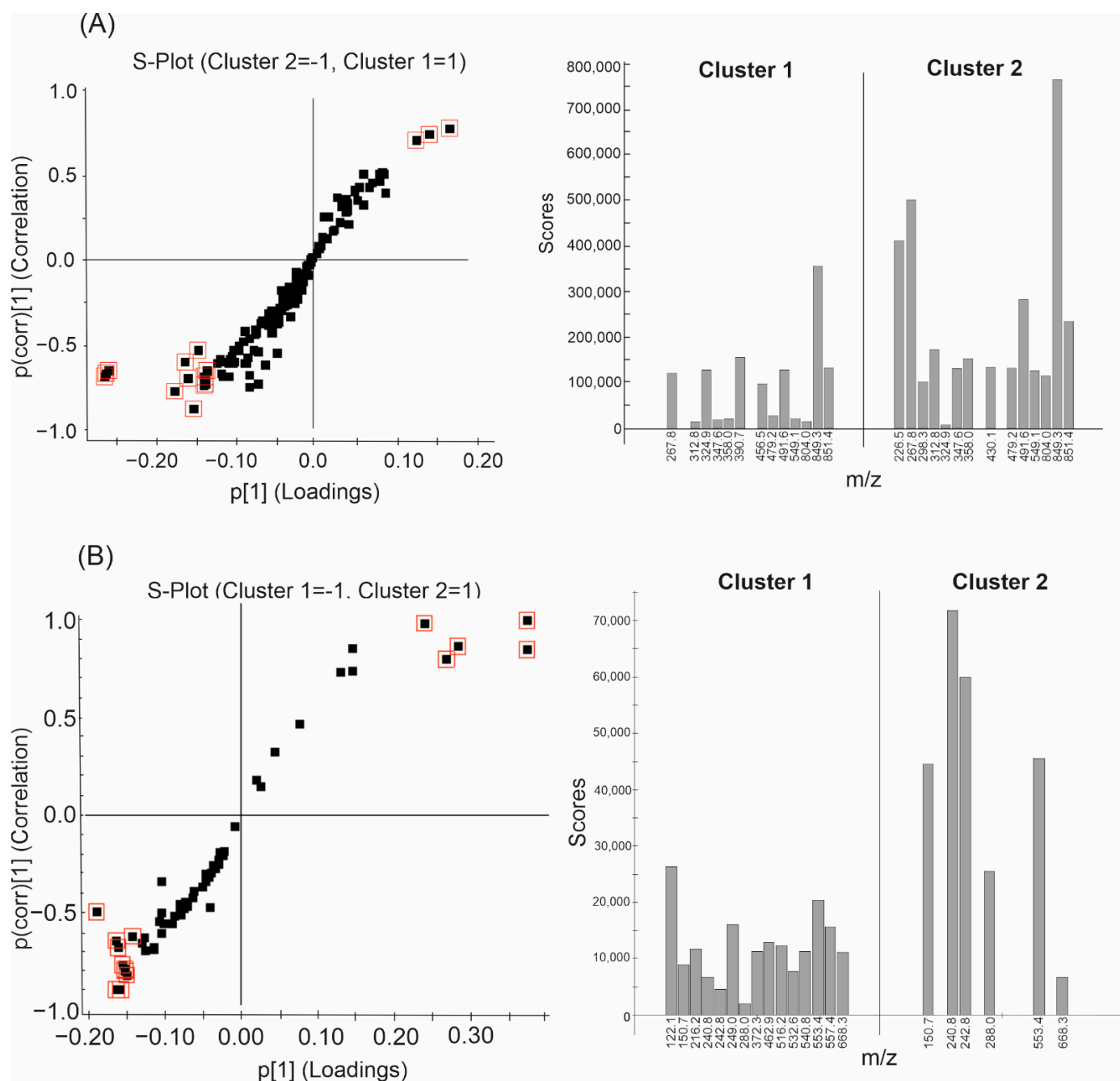


Figure 5. S-plots (left) and normalized mean ion intensities (right) for ions selected in (A) positive mode and (B) negative mode. The highlighted squares correspond to ions with the highest correlation values (VIPs) in their respective clusters; they are highlighted in the histograms to the right of each S-plot. Ions that are repeated in both samples but stand out in relation to their observed intensities are observed in both clusters. Cluster 1: $\text{pH} < 7$; Cluster 2: $\text{pH} \geq 7$.

In contrast, studies that evaluate the metabolic profile of a sample using different solvents or a combination of these during extraction are common [41–43], either for exploring compounds or even chemotaxonomy purposes [41,42,44,45]. In the latter, the approach adopted in this study can be used to determine the robustness of the chemotaxonomic analysis, considering that different strains of the same species can produce different amounts of various compounds that can alter the physicochemical characteristics of the fermented broth, i.e., pH. Consequently, the genotype of the strain can influence the chemical profile of the extraction product [44].

From the point of view of innovation, new bioactive molecules for medical applications need to be increasingly discovered considering emerging diseases and multidrug-resistant microbial strains [46–48]. Therefore, microbial-biomolecule prospecting remains an important niche [47,48]. To this end, non-replicating approaches are increasingly necessary since the quantity and speed at which discoveries are made have both increased due to new methodologies, such as mass spectrometry and its respective databases, which substantially accelerate the ability to chemically characterize compounds [49].

The two metabolic profiles obtained using acidic and basic extraction protocols in this study provide an innovative concept. The data show significant differences that highlight the importance of pH when exploring new biomolecules and facilitate isolation, purification, production, and downstream processes. For example, the ion observed at 430.1 m/z in positive mode (Figure 5A) was only detected in samples from Cluster 2. Therefore, this compound cannot be extracted under conventional extraction conditions that do not adjust the pH to ≥ 7 .

Other approaches that rely on pH can also be adopted to select target molecules. For example, less molecular diversity is obtained at $\text{pH} \geq 7$, which is helpful when purifying target molecules. However, yields are also lower, most likely because most metabolites produced by fungi are acidic in nature [33,39].

3. Materials and Methods

3.1. Endophytic Fungus

The *Diaporthe citri* strain G-01 endophytic fungus was isolated from the leaves of the medicinal *Mikania glomerata* (Spreng.) plant. This microorganism is part of the Collection of Environmental and Endophytic Microorganisms of the Microbial Biotechnology Laboratory at the State University of Maringá (CMEA-LBIOMIC/UEM), Maringá, Paraná, Brazil, and was permanently conserved using the Castellani method.

3.2. Fermentation

Fermentation was performed as described in a previous report that determined the optimal conditions for producing 3-nitropropionic acid (3-NPA) in this strain [34]. The fungus was grown on potato dextrose agar (PDA; Acumedia, Michigan, USA) at pH 6.6, for 7 d at 28 °C. Subsequently, 3–4 plugs (6 mm diameter) were inoculated in 500-mL Erlenmeyer flasks with 250 mL of potato dextrose broth (PD; Acumedia, MI, USA) at pH 7.0 and 28 °C for 22 d.

3.3. Isolating the Crude Extract after Varying the pH

After incubation, the mycelia were removed by filtration through a membrane filter using a Büchner funnel and Kitassato apparatus. The pH of the fermented broth was measured after 22 d of fermentation, which resulted in a pH of approximately 4.0. The pH was adjusted with NaOH or HCl solutions according to Figure 6, resulting in 15 treatments referred to as “PV”, “MV”, and “WV” (in addition to blanks [B]). The following experimental design was used: Five samples were subjected to “plus pH variations” (PVs), in which the pH was adjusted to 2.0 followed by liquid–liquid partitioning, which led to the PV2 samples. The pH of the aqueous phase from the same Erlenmeyer flask was adjusted to 4.0, and extracted to give the PV4 extract. This process was repeated until the pH reached 12.0, which resulted in five extracts per Erlenmeyer flask (PV2, PV4, PV7, PV9, and PV12). Five samples were also subjected to “minus pH variations” (MVs) in a similar manner to that described for the PVs, with pH adjusted from 12.0 to 2.0. Lastly, another five samples were not pH adjusted (“without pH variation”, WV) where the pH of each Erlenmeyer flask was individually adjusted to 2.0, 4.0, 7.0, 9.0, and 12.0 and then partitioned, resulting in one extract per Erlenmeyer flask. Therefore, a single flask was sufficient to extract each of the PV and MV samples, while the WV samples required one flask per extraction. “Blank samples” (B) were prepared using PD broth devoid of inoculum and maintained under the same incubation conditions as the fermented broths. B extraction was performed under the same conditions as those used for the WV samples. All extracts were obtained in duplicate.

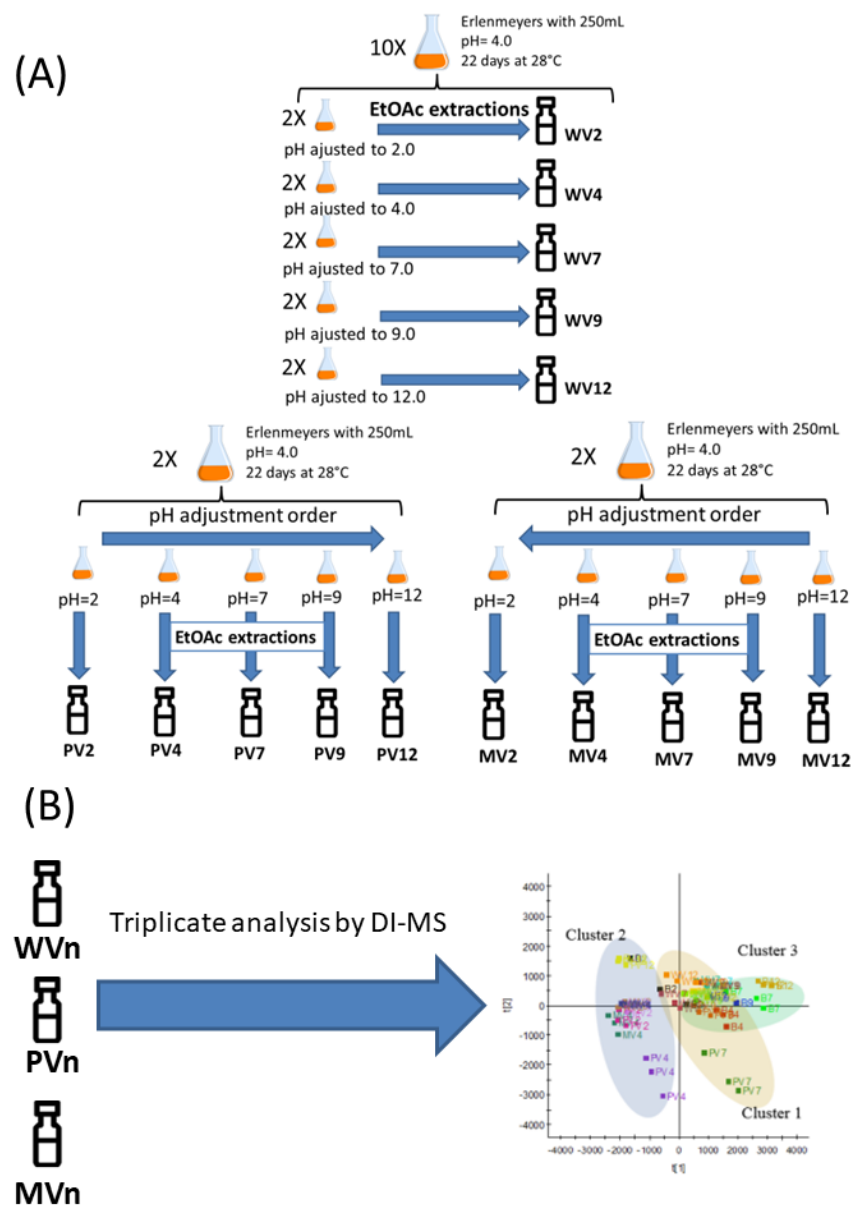


Figure 6. Experimental design: (A) Varying the pH of fermented broth. WV samples: the pH of the fermented broth was adjusted, after which the adjusted broth was extracted with ethyl acetate extraction; the broth was discarded after partitioning. PV and MV fermented broths: pH was adjusted to 2 and 12, respectively, after which they were extracted with ethyl acetate after adjusting the pH to 4 or 9, respectively, without discarding the broth. (B) The obtained vials (two per sample) were analyzed by DI-MS in triplicate.

Liquid–liquid extractions were performed using ethyl acetate (Sigma-Aldrich Corporation, Saint Louis, MO, USA) (1:5 ethyl acetate/broth ratio) in a separating funnel with 250 mL of pH-adjusted fermented broth. This step was repeated four times. The extracts were combined and the solvent was evaporated using a rotary evaporator (Tecnal TE-210, Piracicaba, Brazil) at 40 °C. Yields were variance-analyzed and Skott–Knott tested ($p < 0.05$ was considered to be significant) to determine the best extraction conditions.

3.4. Sample Preparation

The concentration of each extract was adjusted to 1 mg/mL with HPLC-grade methanol (Sigma-Aldrich Corporation, Saint Louis, MO, USA). For electrospray ionization (ESI), each sample was diluted using 10 vol% methanol with either 1% ammonium hydroxide

(Sigma-Aldrich Corporation, Saint Louis, MO, USA) (negative mode) or 1% formic acid (Sigma-Aldrich Corporation, Saint Louis, MO, USA) (positive mode). Each sample was filtered through a 0.45 μm filter and then directly injected (5 μL) into the mass spectrometer (Waters Corporation, Milford, MA, USA). Each sample was analyzed in triplicate.

3.5. Instrumentation

Direct infusion electrospray mass spectrometry (DI-ESI/MS) was performed using a PREMIER/XE[®] Quattro MicroTM API (Waters Corporation, Milford, MA, USA). Data acquisition was controlled using MassLynx version 4.1 software (Waters Corporation, Milford, MA, USA). Prepared samples were injected directly at room temperature into a Rheodyne mass spectrometer (Waters Corporation, Milford, MA, USA). The total run time was 2 min. The desolvation gas-flow rate and source block temperatures were set to 350 and 110 $^{\circ}\text{C}$, respectively. The desolvation gas-flow and cone gas-flow rates were set to 500 and 0.0 L h^{-1} , respectively. Nitrogen gas was used as the drying gas and for misting.

3.6. Data Processing and Multivariate Statistical Analysis

The raw data were first treated using MarkerLynx version 4.1 (Waters Corporation, Milford, MA, USA), where filters were used to remove ions from the mobile phase as well as background noise. Specifically, we used an exclusion list obtained from the mobile phase and a threshold of approximately 10^4 times less than the base peak. The filtered ions were normalized using a Pareto scale. The data were evaluated by analysis of variance (ANOVA; $p < 0.01$ was considered to be significant) and multivariate statistics with unsupervised and supervised approaches: principal component analysis (PCA), hierarchical and non-hierarchical cluster analysis (HCA and k-means, respectively), partial-least-squares discriminant analysis (PLS-DA), orthogonal partial-least-squares discriminant analysis (OPLS-DA), and heatmaps, using the MetaboAnalyst 4.0 online statistical platform, <http://www.metaboanalyst.ca> (accessed on 30 May 2022) [35] and MarkerLynx XS version 3.0.1.0 (Waters Corporation, Milford, MA, USA).

4. Conclusions

We demonstrated that the pH of the fermented broth affects the chemical profile of the metabolic extract. In addition, an extreme pH (i.e., 2 and 12) can highly expressively modify the chemical constituents of a sample in an experimentally inconsistent manner that generates outliers. This study revealed the potential of using a pH gradient (between 4 and 9) to explore secondary fungal metabolites once the analyzed samples had formed clusters based on the pH of the fermented broth ($\text{pH} < 7$ and ≥ 7). Therefore, we propose that extractions at various pH values can provide greater molecular richness in liquid–liquid extraction protocols, affording other molecules that are poorly soluble in a specific solvent under determined conditions, such as the final fermentation process, which may lead to new approaches for exploring fungal metabolites that use this extraction technique.

Supplementary Materials: The following supporting information can be downloaded at: <https://www.mdpi.com/article/10.3390/metabo12080692/s1>, Figure S1: Pareto scaling normalization of the features acquired in positive mode; Figure S2: Pareto scaling normalization of samples acquired in positive mode; Figure S3: Pareto scaling normalization of features acquired in negative mode; Figure S4: Pareto scaling normalization of samples acquired in negative mode; Figure S5: First three principal components to positive data: PC1 (31.9%), PC2 (11.7%), and PC3 (10.8%); Figure S6: Bi-plot analysis of positive-mode-acquired data for PC1 (31.9%) and PC3 (10.8%); Figure S7: First three principal components to negative data: PC1 (32.8%), PC2 (14.2%), and PC3 (9.4%); Figure S8: Bi-plot analysis of negative-mode-acquired data for PC1 (32.8%) and PC3 (9.4%); Figure S9: PLS-DA analysis of samples obtained in negative mode; Figure S10: PLS-DA loadings for samples obtained in negative mode; Figure S11: PLS-DA analysis of samples obtained in positive mode; Figure S12: PLS-DA loadings for samples obtained in positive mode; Figure S13: Heatmap for samples obtained in positive mode; Figure S14: Heatmap for samples obtained in negative mode; Figure S15: PLS-DA analysis of negative-mode data; Figure S16: OPLS-DA analysis of positive-mode data; Figure S17:

OPLS-DA analysis of negative-mode data. The Supplementary Material is organized in a file that includes Figures S1 to S17; Figures S1–S4: Pareto normalization; Figures S5–S8: 3D PCA and Bi-plot analyses; Figures S9–S12: PLS-DA and loadings plots; Figures S13 and S14: Heatmaps from top 25 VIP ions defined by PLS-DA; Figures S15–S17: OPLS-DA analyses.

Author Contributions: Conceptualization, J.C.P.; Methodology, J.C.P., M.A.d.S.R., C.Z.F.-P. and E.C.M.; software: J.C.P., M.A.d.S.R., C.Z.F.-P. and E.C.M.; validation, J.C.P. and E.C.M.; formal analysis, M.A.d.S.R. and E.C.M.; investigation, C.Z.F.-P.; writing—original draft preparation, J.C.P. and E.C.M.; writing—review and editing, J.L.A. and H.C.G.; and supervision, J.A.P. All authors have read and agreed to the published version of the manuscript.

Funding: This research was funded by the Coordenação de Aperfeiçoamento de Pessoal de Nível Superior (CAPES) (Financial code: 001), CNPq (307603/2017-2), and SETI-UGF (TC n.65/2018).

Institutional Review Board Statement: Not applicable.

Informed Consent Statement: Not applicable.

Data Availability Statement: The data presented in this study are available in Supplementary Materials at [doi:10.5281/zenodo.6613511].

Acknowledgments: We thank the Universidade Estadual de Maringá and the Universidade Federal do Paraná—Campus Jandaia do Sul for structural and equipment supports. We also thank the Graduate Program in Environmental Biotechnology to support and viability of this study.

Conflicts of Interest: The authors declare no conflict of interest.

References

1. Pamphile, J.A.; Ribeiro, M.A.S.; Polonio, J.C. Secondary Metabolites of Endophyte Fungi: Techniques and Biotechnological Approaches. In *Diversity and Benefits of Microorganisms from the Tropics*, 1st ed.; Azevedo, J.L., Quecine, M.C., Eds.; Springer: Cham, Switzerland, 2017; pp. 185–206. [\[CrossRef\]](#)
2. Schulz, B.; Boyle, C. The endophytic continuum. *Mycol. Res.* **2015**, *109*, 661–686. [\[CrossRef\]](#)
3. Kusari, S.; Hertweck, C.; Spiteller, M. Chemical ecology of endophytic fungi: Origins of secondary metabolites. *Chem. Biol.* **2012**, *19*, 792–798. [\[CrossRef\]](#)
4. Ludwig-Müller, J. Plants and endophytes: Equal partners in secondary metabolite production? *Biotechnol. Lett.* **2015**, *37*, 1325–1334. [\[CrossRef\]](#)
5. Stierle, A.; Strobel, G.; Stierle, D. Taxol and taxane production by *Taxomyces andreanae*, an endophytic fungus of Pacific yew. *Science* **1993**, *260*, 214–221. [\[CrossRef\]](#)
6. Schulz, B.; Boyle, C.; Draeger, S.; Römmert, A.K.; Krohn, K. Endophytic fungi: A source of novel biologically active secondary metabolites. *Mycol. Res.* **2002**, *106*, 996–1004. [\[CrossRef\]](#)
7. Chagas, F.O.; Caraballo-Rodríguez, A.M.; Pupo, M.T. Endophytic Fungi as a Source of Novel Metabolites. In *Endophytic Fungi as a Source of Novel Metabolites in Biosynthesis and Molecular Genetics of Fungal Secondary Metabolites*; Martin, J.-F., Garcia-Estrada, C., Zeilinger, S., Eds.; Springer: New York, NY, USA, 2015; pp. 123–176.
8. Dzoyem, J.P.; Melong, R.; Tsamo, A.T.; Maffo, T.; Kapche, D.G.; Ngadjui, B.T.; McGaw, L.J.; Eloff, J.N. Cytotoxicity, antioxidant and antibacterial activity of four compounds produced by an endophytic fungus *Epicoccum nigrum* associated with *Entada abyssinica*. *Rev. Bras. Farmacogn.* **2017**, *27*, 251–253. [\[CrossRef\]](#)
9. Li, C.; Sarotti, A.M.; Yoshida, W.; Cao, S. Two new polyketides from Hawaiian endophytic fungus *Pestalotiopsis* sp. FT172. *Tetrahedron Lett.* **2018**, *59*, 42–45. [\[CrossRef\]](#)
10. Rajivgandhi, G.; Muneeswaran, T.; Maruthupandy, M.; Ramakritinan, C.M.; Saravanan, K.; Ravikumar, V.; Manoharan, N. Antibacterial and anticancer potential of marine endophytic actinomycetes *Streptomyces coeruleorubidus* GRG 4 (KY457708) compound against colistin resistant uropathogens and A549 lung cancer cells. *Microb. Pathog.* **2018**, *125*, 325–335. [\[CrossRef\]](#)
11. Rojas-Solis, D.; Zetter-Salmón, E.; Contreras-Pérez, M.; del Carmen Rocha-Granados, M.; Macías-Rodríguez, L.; Santoyo, G. *Pseudomonas stutzeri* E25 and *Stenotrophomonas maltophilia* CR71 endophytes produce antifungal volatile organic compounds and exhibit additive plant growth-promoting effects. *Biocatal. Agric. Biotechnol.* **2018**, *13*, 46–52. [\[CrossRef\]](#)
12. Wang, A.; Li, P.; Zhang, X.; Han, P.; Lai, D.; Zhou, L. Two new anisic acid derivatives from endophytic fungus *Rhizopycnis vagum* Nitaf22 and their antibacterial activity. *Molecules* **2018**, *23*, 591. [\[CrossRef\]](#)
13. Tan, R.X.; Zou, W.X. Endophytes: A rich source of functional metabolites. *Nat. Prod. Rep.* **2001**, *18*, 448–459. [\[CrossRef\]](#)
14. Meng, X.; Mao, Z.; Lou, J.; Xu, L.; Zhong, L.; Peng, Y.; Zhou, L.; Wang, M. Benzopyranones from the endophytic fungus *Hyalodendriella* sp. Ponipodef12 and their bioactivities. *Molecules* **2012**, *17*, 11303–11314. [\[CrossRef\]](#)
15. Yang, H.Y.; Gao, Y.H.; Niu, D.Y.; Yang, L.Y.; Gao, X.M.; Du, G.; Hu, Q.-F. Xanthone derivatives from the fermentation products of an endophytic fungus *Phomopsis* sp. *Fitoterapia* **2013**, *91*, 189–193. [\[CrossRef\]](#)

16. Ye, Y.-Q.; Xia, C.-F.; Yang, J.-X.; Qin, Y.; Zhou, M.; Gao, X.-M.; Yang, H.-Y.; Li, X.-M.; Hu, Q.-F. Isocoumarins from the fermentation products of an endophytic fungus of *Aspergillus versicolor*. *Phytochem. Lett.* **2014**, *10*, 215–218. [[CrossRef](#)]
17. Chagas, F.O.; Dias, L.G.; Pupo, M.T. New perylenequinone derivatives from the endophytic fungus *Alternaria tenuissima* SS77. *Tetrahedron Lett.* **2016**, *57*, 3185–3189. [[CrossRef](#)]
18. Liangsakul, J.; Srisurichan, S.; Pornpakakul, S. Anthraquinone–steroids, evanthrasterol A and B, and a meroterpenoid, emericellic acid, from endophytic fungus, *Emericella varicolor*. *Steroids* **2016**, *106*, 78–85. [[CrossRef](#)]
19. Wang, M.; Sun, Z.-H.; Chen, Y.-C.; Liu, H.-X.; Li, H.-H.; Tan, G.-H.; Li, S.-N.; Guo, X.-L.; Zhang, W.-M. Cytotoxic cochlioquinone derivatives from the endophytic fungus *Bipolaris sorokiniana* derived from *Pogostemon cablin*. *Fitoterapia* **2016**, *110*, 77–82. [[CrossRef](#)]
20. Kusari, S.; Singh, S.; Jayabaskaran, C. Rethinking production of Taxol[®] (paclitaxel) using endophyte biotechnology. *Trends biotechnol.* **2014**, *32*, 304–311. [[CrossRef](#)]
21. Schulz, B.; Sucker, J.; Aust, H.J.; Krohn, K.; Ludewig, K.; Jones, P.G.; Döring, D. Biologically active secondary metabolites of endophytic *Pezizula* species. *Mycol. Res.* **1995**, *99*, 1007–1015. [[CrossRef](#)]
22. Taechowisan, T.; Lu, C.; Shen, Y.; Lumyong, S. Secondary metabolites from endophytic *Streptomyces aureofaciens* CMUAc130 and their antifungal activity. *Microbiology* **2005**, *151*, 1691–1695.
23. Kjer, J.; Debbab, A.; Aly, A.H.; Proksch, P. Methods for isolation of marine-derived endophytic fungi and their bioactive secondary products. *Nat. Protoc.* **2010**, *5*, 479. [[CrossRef](#)]
24. Mendonca, A.N.; Felipe, B.H.M.P.; Lemes, R.M.L.; Ruiz, A.L.T.G.; de Carvalho, J.E.; Ikegaki, M. Potential antimicrobial and antiproliferative activity of the crude extract of the endophytic fungus *Rhizoctonia* sp. from *Annona crassiflora*. *Afr. J. Pharm. Pharmacol.* **2015**, *9*, 327–332.
25. Kumar, A.; Jha, K.P.; Kumar, R.; Kumar, K.; Sedolkar, V. Antibacterial activity, phytochemical and enzyme analysis of crude extract of endophytic fungus, *Alternaria* sp. isolated from an ethnobotanical medicinal plant *Tridax procumbens*. *Int. J. Pharma Phytochem. Res.* **2015**, *7*, 1111–1115.
26. Nasr, H.M.; Abdel-Ghany, R.O.; Mousa, S.A.; Alasmaey, M.; Atalla, A.A. Biological activity of crude extracts of endophytic *Fusarium oxysporum* and its chemical composition by gas chromatography–mass spectrometry. *Elixir Org. Chem.* **2018**, *117*, 50565–50568.
27. Yu, H.; Zhang, L.; Li, L.; Zheng, C.; Guo, L.; Li, W.; Sun, P.; Qin, L. Recent developments and future prospects of antimicrobial metabolites produced by endophytes. *Microbiol. Res.* **2010**, *165*, 437–449. [[CrossRef](#)]
28. Bogner, C.W.; Kamdem, R.S.; Sichtermann, G.; Matthäus, C.; Hölscher, D.; Popp, J.; Proksch, P.; Grundler, F.M.W.; Schouten, A. Bioactive secondary metabolites with multiple activities from a fungal endophyte. *Microb. Biotechnol.* **2017**, *10*, 175–188. [[CrossRef](#)]
29. Maciá-Vicente, J.G.; Shi, Y.N.; Cheikh-Ali, Z.; Grün, P.; Glynou, K.; Kia, S.H.; Piepebring, M.; Bode, H.B. Metabolomics-based chemotaxonomy of root endophytic fungi for natural products discovery. *Environ. Microbiol.* **2018**, *20*, 1253–1270. [[CrossRef](#)]
30. Brakhage, A.A. Regulation of fungal secondary metabolism. *Nat. Rev. Microbiol.* **2013**, *11*, 21–32. [[CrossRef](#)]
31. Sharma, V.; Singamaneni, V.; Sharma, N.; Kumar, A.; Arora, A.; Kushwaha, M.; Bhushan, S.; Jaglan, S.; Gupta, P. Valproic acid induces three novel cytotoxic secondary metabolites in *Diaporthe* sp., an endophytic fungus from *Datura innoxia* Mill. *Bioorg. Med. Chem. Lett.* **2018**, *28*, 2217–2221. [[CrossRef](#)]
32. Martins, C.R.; Lopes, W.A.; Andrade, J.B.D. Organic compound solubility. *Quim. Nova* **2013**, *36*, 1248–1255. [[CrossRef](#)]
33. Nielsen, K.F.; Larsen, T.O. The importance of mass spectrometric dereplication in fungal secondary metabolite analysis. *Front. Microbiol.* **2015**, *6*, 71. [[CrossRef](#)]
34. Polonio, J.C.; Ribeiro, M.A.S.; Rhoden, S.A.; Sarragiotto, M.H.; Azevedo, J.L.; Pamphile, J.A. 3-Nitropropionic acid production by the endophytic *Diaporthe citri*: Molecular taxonomy, chemical characterization, and quantification under pH variation. *Fungal Biol.* **2016**, *120*, 1600–1608. [[CrossRef](#)]
35. Chong, J.; Soufan, O.; Li, C.; Caraus, I.; Li, S.; Bourque, G.; Wishart, D.S.; Xia, J. MetaboAnalyst 4.0: Towards more transparent and integrative metabolomics analysis. *Nucleic Acids Res.* **2018**, *46*, w486–w494. [[CrossRef](#)]
36. Aksenov, A.A.; da Silva, R.; Knight, R.; Lopes, N.P.; Dorrestein, P.C. Global chemical analysis of biology by mass spectrometry. *Nat. Rev. Chem.* **2017**, *1*, 0054. [[CrossRef](#)]
37. Eriksson, L.; Johansson, E.; Kettaneh-Wold, N.; Wikström, C.; Wold, S. *Design of Experiments: Principles and Applications*; Umetrics: Umeå, Sweden, 2008.
38. Rundberget, T.; Skaar, I.; O'brien, O.; Flåøyen, A. Penitrem and thomitrem formation by *Penicillium crustosum*. *Mycopathologia* **2004**, *157*, 349–357. [[CrossRef](#)]
39. Månsson, M.; Phipps, R.K.; Gram, L.; Munro, M.H.; Larsen, T.O.; Nielsen, K.F. Explorative solid-phase extraction (E-SPE) for accelerated microbial natural product discovery, dereplication, and purification. *J. Nat. Prod.* **2010**, *73*, 1126–1132. [[CrossRef](#)]
40. Li, Q.; Wang, D.; Wu, Y.; Li, W.; Zhang, Y.; Xing, J.; Su, Z. One step recovery of succinic acid from fermentation broths by crystallization. *Sep. Purif. Technol.* **2010**, *72*, 294–300. [[CrossRef](#)]
41. Gao, Z.; Shen, P.; Lan, Y.; Cui, L.; Ohm, J.B.; Chen, B.; Rao, J. Effect of alkaline extraction pH on structure properties, solubility, and beany flavor of yellow pea protein isolate. *Food Res. Int.* **2020**, *131*, 109045. [[CrossRef](#)]
42. Pelo, S.P.; Adebo, O.A.; Green, E. Chemotaxonomic profiling of fungal endophytes of *Solanum mauritianum* (alien weed) using gas chromatography high resolution time-of-flight mass spectrometry (GC-HRTOF-MS). *Metabolomics* **2021**, *17*, 43. [[CrossRef](#)]

43. Want, E.J.; O'Maille, G.; Smith, C.A.; Brandon, T.R.; Uritboonthai, W.; Qin, C.; Trauger, S.A.; Siuzdak, G. Solvent-dependent metabolite distribution, clustering, and protein extraction for serum profiling with mass spectrometry. *Anal. Chem.* **2006**, *78*, 743–752. [[CrossRef](#)]
44. Frisvad, J.C.; Andersen, B.; Thrane, U. The use of secondary metabolite profiling in chemotaxonomy of filamentous fungi. *Mycol. Res.* **2008**, *112*, 231–240. [[CrossRef](#)]
45. Aliferis, K.A.; Cubeta, M.A. Chemotaxonomy of fungi in the *Rhizoctonia solani* species complex performing GC/MS metabolite profiling. *Metabolomics* **2013**, *9*, S159–S169. [[CrossRef](#)]
46. El Omari, N.; Guaouguaou, F.E.; Bouyahya, A. Natural Bioactive Compounds from Medicinal Plants as Antibacterial Drugs: Mechanism Insights and Clinical Perspectives. *Curr. Top. Med. Chem.* **2022**, *22*, 1093–1103. [[CrossRef](#)]
47. De Simeis, D.; Serra, S. Actinomycetes: A never-ending source of bioactive compounds—An overview on antibiotics production. *Antibiotics* **2021**, *10*, 483. [[CrossRef](#)]
48. Rani, A.; Saini, K.C.; Bast, F.; Varjani, S.; Mehariya, S.; Bhatia, S.K.; Sharma, N.; Funk, C. A review on microbial products and their perspective application as antimicrobial agents. *Biomolecules* **2021**, *11*, 1860. [[CrossRef](#)]
49. Jude, S.; Gopi, S. Dereplication: HRMS in Phytochemical Analysis. In *High-Resolution Mass Spectroscopy for Phytochemical Analysis*; Gopi, S., Amalraj, A., Jude, S., Eds.; Apple Academic Press: Waretown, NJ, USA, 2021; pp. 45–66.